Available online at www.sciencedirect.com
SCIENCE DIRECT
Applied Catalysis A: General 283 (2005) 1–8
APPLIED CATALYSIS A: GENERAL
www.elsevier.com/locate/apcata

Novel tungsten-containing mesoporous HMS material: its synthesis, characterization and catalytic application in the selective oxidation of cyclopentene to glutaraldehyde by aqueous H_2O_2

Xin-Li Yang[a], Wei-Lin Dai[a,*], Hui Chen[a], Jian-Hua Xu[a], Yong Cao[a], Hexing Li[b], Kangnian Fan[a,*]

[a]*Department of Chemistry and Shanghai Key Laboratory of Molecular Catalysis and Innovative Materials, Fudan University, Shanghai 200433, PR China*
[b]*Department of Chemistry, Shanghai Normal University, Shanghai 200234, PR China*

Received 16 July 2004; received in revised form 21 November 2004; accepted 21 December 2004
Available online 21 January 2005

Abstract

Tungsten-containing hexagonal mesoporous silica (HMS) has been synthesized by using dodecylamine as template at room temperature. The as-prepared novel material is very active as a catalyst for the selective oxidation of cyclopentene (CPE) to glutaraldehyde (GA) with environmentally benign hydrogen peroxide as the oxidant. Tungsten species could stably exist in the silica-based matrix of HMS up to a Si/W molar ratio of 30, as determined by X-ray diffraction (XRD), laser Raman spectroscopy, and FT-IR. Proper content of tungsten species and its high dispersion account for its high activity. Complete conversion of cyclopentene and very high yield of glutaraldehyde (~76.3%) are obtained over the W-HMS catalyst with a Si/W molar ratio at 30. Furthermore, almost no tungsten species are leached into the reaction solution, enabling the catalyst to be employed for many reaction cycles without dramatic deactivation.

Keywords: Cyclopentene; Glutaraldehyde; H_2O_2; Tungsten; HMS; W-HMS

1. Introduction

Glutaraldehyde (GA) has been used extensively for disinfection and sterilization in many areas. However, the commercial preparation method from propenal and vinyl ethyl ether is now being restricted by its complicated preparation process and expensive raw materials [1,2]. This has resulted in the high price of GA and has constrained its wide use in other fields, such as the tanning process of leather, environmental protection, water treatment, and oil field. The preparation of GA in a more convenient and economical way has been an important objective for many researchers. An alternative way to produce GA is from the selective oxidation of cyclopentene (CPE) with environmentally benign aqueous H_2O_2 as the oxidant, since a great quantity of CPE could be easily obtained by the selective hydrogenation of cyclopentadiene. The direct synthesis of GA from CPE appears to be an attractive way of utilizing cyclopentadiene, a main by-product of the C-5 fraction in the petrochemical industry [3,4].

Recently, several W-containing homogeneous catalysts have been reported as good catalysts for GA preparation [4–7]. However, the difficulties of separating and recovering the catalysts from the product mixture in the homogeneous process made them impractical for industrial production process. One of the most promising approaches is to design a heterogeneous W-containing catalyst. Up to now, we have already designed four heterogeneous W-containing catalysts (WO_3/SiO_2, WO_3/TiO_2-SiO_2, W-MCM-41 and W-SBA-15) [8–12]. Among these catalysts, W-MCM-41 shows the highest catalytic

* Corresponding authors. Tel.: +86 215 566 4678; fax: +86 21 65642978.
E-mail addresses: wldai@fudan.edu.cn (W.-L. Dai), knfan@fudan.edu.cn (K. Fan).

0926-860X/$ – see front matter © 2004 Elsevier B.V. All rights reserved.
doi:10.1016/j.apcata.2004.12.029

activity and GA yield; W-SBA-15 is still being investigated; so far it also shows good performance in this reaction. All the previous works show that high surface area and large and uniform pore size of the support could be helpful to the catalytic performance of GA preparation. Hexagonal mesoporous silica (HMS) synthesized by the assembly pathway of hydrogen-bonding interactions between neutral primary alkylamine and neutral inorganic precursors at room temperature [13] also accords well with the above requirements. This is because HMS has very high surface areas, up to 1000 $m^2 g^{-1}$ or even more, uniform pore size, ultra-high thermal stability (up to 1073 K) and strong sorption capacities for hydrocarbons. These features extend its applications in the field of catalysis, molecular sieving, and supports. Moreover, HMS possesses a much thicker framework wall, smaller domain size with short channels, and larger textual mesoporosity [13–16]; these properties are distinguishable from those of MCM-41, and provide better transport channels for reactants to access the active centers and better diffusion channels for products to move out than their MCM-41 analogs.

The framework of HMS can be uniformly modified by transition metal ions, such as Ti^{4+}, Al^{3+}, Zr^{4+}, V^{5+}, Cu^{2+}, Cr^{6+}, Mn^{2+}, and Nb^{5+} [17–22]. These transition metal-modified HMS samples usually show high activity in many organic reactions [13,23,24]. However, there are no reports concerning the preparation of a W^{6+} substituting HMS material. Therefore, it may be possible to prepare W-containing HMS as a heterogeneous catalyst with better catalytic behavior for GA preparation. Here, for the first time, we report a novel heterogeneous catalyst, W-HMS. The preparation of GA from the oxidation of CPE is done by using aqueous H_2O_2 as the oxidant; this in turn is prepared by the isomorphous substitution of silicon by tungsten. The as-prepared W-HMS heterogeneous catalyst showed much higher activity and selectivity in the selective oxidation of CPE to GA. The conversion of CPE is 100% and the yield of GA is 76.3%, ca. 4% higher than that of W-MCM-41. Moreover, the leaching of tungsten in the reaction mixture was extremely low (<1 ppm), making it possible for this catalyst to be a promising candidate for the industrial production of GA.

2. Experimental

2.1. Catalyst preparation

W-HMS samples were synthesized at room temperature by using dodecylamine as surfactant molecule. In a typical preparation process, 5.04 g of dodecylamine was added to a solution containing 53.3 mL of H_2O, 33.6 mL of ethanol and 2 mL of HCl (2 M). The mixture was stirred until it became homogeneous. Then 23 mL of tetraethyl orthosilicate (TEOS) in 20 mL ethanol and the required amount of aqueous sodium tungstate solution ($NaWO_4 \cdot 2H_2O$, 0.2 M) were simultaneously and quickly added into the mixture under vigorous stirring. The resulting gel was stirred for 15 min and aged for 18 h at room temperature (~298 K). The precipitate was recovered by filtration, washed with distilled water, dried at room temperature, and finally calcined at 873 K in air for 5 h. Pure HMS was prepared for comparison, following a procedure similar to that reported by Tanev et al. [13].

2.2. Catalyst characterization

The small-angle X-ray powder diffraction (SAXS) patterns were recorded on Rigaku D/max-rB spectrometer with Cu Kα radiation, which was operated at 60 mA and 40 kV. The wide-angle X-ray powder diffraction (WAXS) patterns were recorded on a Bruker D8 Advance spectrometer with Cu Kα radiation, which was operated at 40 mA and 40 kV. The laser Raman experiment was performed by using a Jobin Yvon Dilor Labram I Raman spectrometer equipped with a holographic notch filter, a CCD detector and He–Ne laser radiating at 632.8 nm. The specific surface areas, the pore volumes and the mean pore diameters of the samples were measured and calculated according to the BET method with a Micromeritics Tristar BET spectrometer with liquid nitrogen at 77 K. Scanning electron micrographs were obtained using a Philips XL 30 spectrometer. The samples were deposited on a sample holder with a piece of adhesive carbon tape and were then sputtered with a thin film of gold. Transmission electron micrographs (TEM) were obtained on a Joel JEM 2010 scan-transmission electron microscope. The samples were supported on carbon-coated copper grids for the experiment. The FT-IR measurements were carried out with a Nicolet Model 205 spectrometer, using KBr pellet technique. The tungsten content in W-HMS was determined by inductively coupled argon plasma (ICP, IRIS Intrepid, Thermo Elemental Company) after solubilization of the samples in HF:HCl solutions.

2.3. Activity test

The activity test was performed at 308 K for 24 h with magnetic stirring in a closed 100 mL regular glass reactor using 50 wt.% aqueous H_2O_2 as oxygen-donor and *tert*-butanol (*t*-BuOH) as the solvent. In a typical experiment, 5 mL of cyclopentene, 50 mL of *t*-BuOH, and 0.9 g of the W-HMS (30) were introduced into the regular glass reactor at 308 K with vigorous stirring. The reaction was started by adding 7 mL of 50 wt.% aqueous H_2O_2 into the mixture and was kept stirring for 24 h (the initial molar ratio of H_2O_2 to CPE was kept at 2.0). The quantitative analysis of the reaction products was done by the method of GC and the determination of different products in the reaction mixture was performed by means of GC–MS. Details can be found elsewhere [9].

3. Results and discussion

3.1. Structural characteristics of the catalysts

The SAXS patterns of various samples are shown in Fig. 1. Each sample exhibits an intense diffraction peak corresponding to the (1 0 0) plane at 2θ of 2–3°, typical characteristic of HMS materials, except for the one at Si/W = 20. As the transition metal tungsten is incorporated into the bulk of HMS, the $d_{1\,0\,0}$ spacing shifts to a lower diffraction angle and become slightly broader. The intensity of the reflection corresponding to the (1 0 0) plane decreases with the decrease of the Si/W molar ratio as compared with the corresponding pure HMS, as shown in Fig. 1(a–d). All such phenomena suggest the presence of progressive expansion of the latticed-spacings upon the incorporation of W heteroatoms. Further decrease of the Si/W molar ratio (20) leads to the partial collapse of the mesoporous structure, as shown in Fig. 1(e). And also, the BET surface area and pore volume of W-HMS samples are lower than that of pure HMS, but the pore size is slightly higher than that of pure HMS, as shown in Table 1. It is found that the BET surface areas of those samples at Si/W molar ratio of 20 and 30 are only 60% as compared to surface area of the pure sample while that with Si/W molar ratio at 50 still possesses 83% of the BET area of the pure sample, indicating the great influence of the added heteroatoms. As to the results of pore volumes, similar phenomena can also be observed. That is, higher content of tungsten will reduce the corresponding pore volume abruptly. If the amount of the added tungsten heteroatoms reaches a much higher value, the typical mesoporous structure cannot be kept. The inflection point at $P/P_0 = 0.25$–0.35 in N_2 adsorption isotherm (not shown) indicates that the W-HMS samples possess regular mesopores, except for the one at Si/W = 20, suggesting that there is no regular mesoporous structure in the W-HMS sample at Si/W = 20. Table 1 also lists the actual metal amounts in the products measured by ICP method. The results are very well consistent with the added metal amounts in the as-prepared samples, suggesting that most of the added tungsten heteroatoms are embedded into the lattice of the HMS bulk.

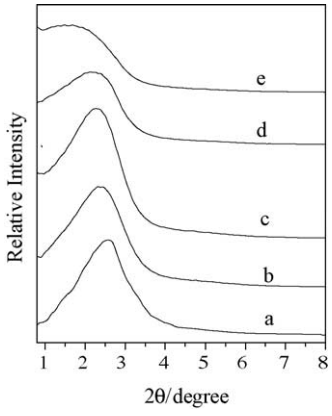

Fig. 1. Small-angle XRD patterns of pure HMS and W-HMS. (a) Pure HMS; (b) W-HMS, Si/W = 50; (c) 40; (d) 30; and (e) 20.

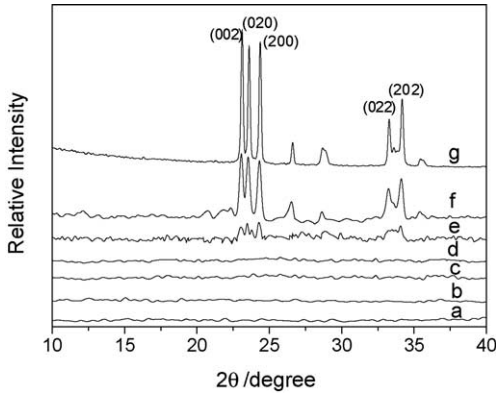

Fig. 2. Wide-angle XRD patterns of bulk WO_3 and W-HMS samples at different Si/W ratios. (a) W-HMS, Si/W = 50; (b) 40; (c) 30; (d) 30, calcined at 873 K after 10 reaction cycles; (e) 30, after 10 reaction cycles; (f) 20; and (g) crystalline WO_3.

The WAXS patterns of various samples are shown in Fig. 2, and that of pure crystalline WO_3 is also presented for comparison. In all the WAXS patterns of the samples with Si/W molar ratios larger than or equal to 30, no peaks corresponding to crystalline WO_3 are observed, indicating the absence of agglomerated crystalline WO_3 in those catalysts. Also, no WO_3 crystals or amorphous congeries could be found on the surface of those samples, as confirmed by SEM, suggesting that WO_3 is totally incorporated into the lattice of the HMS structure. When the Si/W molar ratio is equal to 20, strong characteristic peaks of crystalline WO_3 appear, as shown in Fig. 2(f), suggesting that WO_3 begins to congregate at this Si/W molar ratio. In Fig. 2, the used and the regenerated W-HMS (30) after 10 reaction cycles are also shown as (e) and (d), respectively. It is easy to find that there are weak peaks ascribed to crystalline WO_3 appeared in the X-ray diffraction (XRD) pattern for the used catalyst, suggesting the presence of the crystallization of tungsten species in the W-HMS (30) sample during the long-term reaction process. After regeneration with 873 K treatment in air for 2 h, the weak peaks disappear, indicating that the re-dispersion of tungsten species has happened, as confirmed by TEM. This result shows that the tungsten species in W-HMS material is mobilizable under the reaction conditions. It is also very interesting that the tungsten species accumulated on the surface of the catalyst can be embedded into the lattice of HMS again after treatment with high temperature because of the driving force of thermodynamics since the high dispersion of tungsten oxide is very stable [25]. Similar conclusion can also be deduced according to the results from X-ray photoelectron spectroscopy (XPS). That is, the surface ratio of W/Si of the deactivcated catalyst is smaller than that of the fresh catalyst, however, this ratio will revert to its fresh state after the process of regeneration. Therefore, this novel catalyst may show much longer lifetime for its further use in industry.

Table 1
Physico-chemical parameters of various samples

Samples	Si/W[a] (mol)	Si/W[b] (mol)	Surface area (m^2/g)	Pore volume (cm^3/g)	Pore diameter (nm)
HMS (∞)	∞	∞	1160	1.0	2.6
W-HMS (50)	50	52.0	960	0.8	2.9
W-HMS (40)	40	41.9	846	0.8	3.2
W-HMS (30)	30	33.6	703	0.7	3.1
W-HMS (20)	20	21.9	692	0.7	3.5

[a] Stoichiometric ratio in gel.
[b] Measured by ICP.

Scanning electron microscopy with energy diffraction (SEM–EDX) measurements also confirm that no agglomerated WO_3 could be observed on the surface of W-HMS sample (Si/W = 30) and that the W-HMS sample (Si/W = 30) retains the morphology similar to that of pure HMS, as shown in Fig. 3. The result suggests that 12.9 wt.% WO_3 (corresponding to Si/W ratio = 30) does not influence its morphology obviously. Transmission electron microscopy (TEM) results show that W-HMS (30) still possesses the typical wormhole structures of HMS material assembled from long alkyl chain neutral amines as surfactants (Fig. 4) [24], meaning that tungsten species are highly dispersed or imbedded in the silica matrix. However, microcrystalline WO_3 species appear on the surface after 10 reaction cycles (Fig. 4c), as confirmed by EDX. The WO_3 particle size is ca. 40 nm, much larger than that estimated from W (0 0 2) line (3.6 nm) calculated from the widening of the XRD peaks (Fig. 2e), suggesting that the WO_3 particle consists of many WO_3 microcrystalline. After calcination at 873 K for 2 h, those microcrystalline WO_3 species disappear again (Fig. 4d), indicating the catalyst can be easily regenerated and the high dispersion of tungsten species is thermodynamically stable.

The Raman spectra, as shown in Fig. 5, provide additional information about the WO_3 structure of the W-HMS samples. In comparison with the standard octahedral crystalline WO_3 (Fig. 5h), no Raman bands attributed to the octahedral crystalline WO_3, at ca. 804, 714, 327 and 267 cm^{-1} [26] are observed for W-HMS (Si/W > 30, see Fig. 5(b–d)). The Raman bands in Fig. 5(b–d) are very similar to those of the pure HMS (Fig. 5a). Fig. 5(g) shows the Raman spectra of W-HMS samples with much higher content of tungsten species (Si/W = 20). Obvious Raman bands assigned to crystalline WO_3 can be observed, illustrating that certain high content of tungsten species would result in the agglomeration of microcrystalline WO_3 on the surface. Hence, a proper content of tungsten species is necessary for its high dispersion and for the stability of special mesoporous structure of HMS. In Fig. 5, the Raman bands for the used catalyst and the regenerated one corresponding to that in the WAXS patterns are also shown as (e) and (f), respectively. Similar to the result observed in XRD, only a little amount of WO_3 is observed with the used catalyst. In addition, in the region of 950–1000 cm^{-1}, new Raman bands corresponding to organic compounds appear, implying that there is adsorbed organic contaminant on the surface of the used catalyst, which was then confirmed by means of XPS measurement. This may be one of the reasons why the activity will be decreased after long-term reaction. After the sample is treated at high temperature, those Raman bands disappear, indicating that this novel catalyst can be totally regenerated to its fresh state after simple thermal treatment.

The FT-IR spectra of the samples are shown in Fig. 6. All the samples exhibit the symmetric stretching vibration band at around 810 cm^{-1} and the anti-symmetric vibration band at around 1100 cm^{-1} for the tetrahedral SiO_4 structure units. No typical IR band located at around 960 cm^{-1} can be observed for the pure HMS. However, W-HMS exhibits an infrared band at around 960 cm^{-1}, similar to that of W-MCM-41 [10,27]. The band at around 960 cm^{-1} has been widely used to characterize the incorporation of metal ions

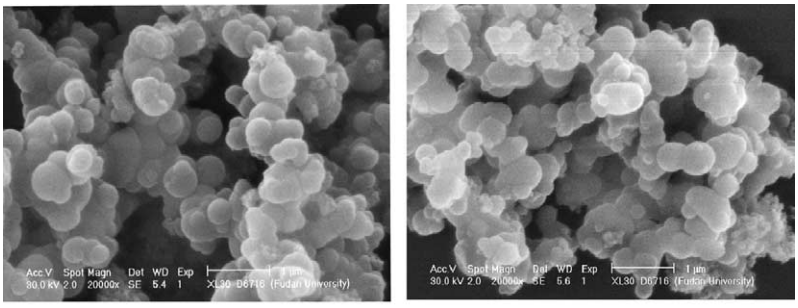

(a) (b)

Fig. 3. Scanning electron micrographs of pure HMS and W-HMS (Si/W = 30). (a) Pure HMS; and (b) W-HMS, Si/W = 30.

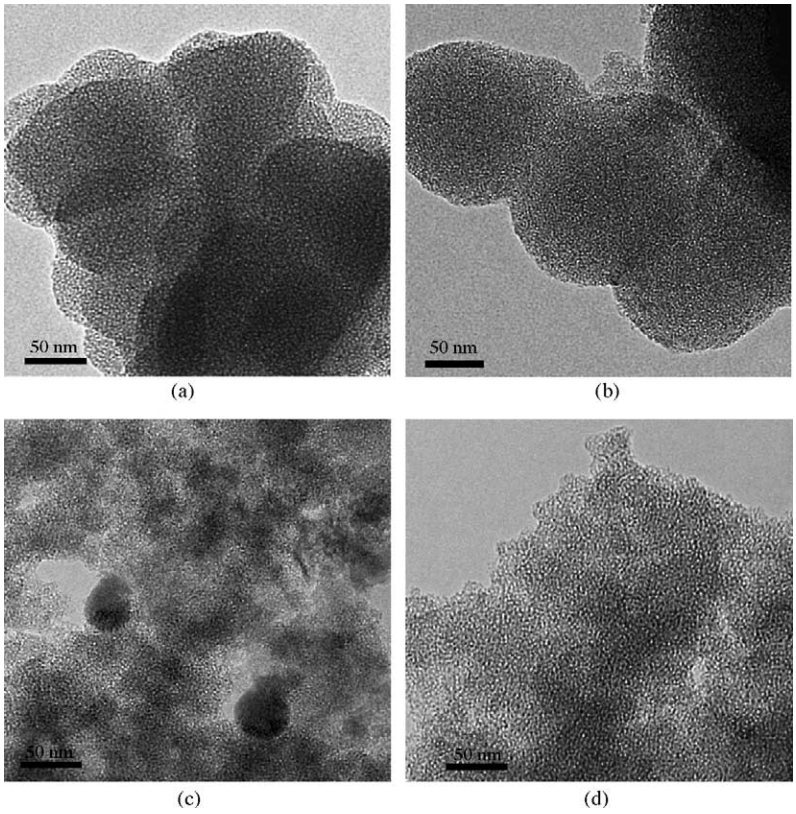

Fig. 4. Transmission electron micrographs of HMS and W-HMS (Si/W = 30). (a) Pure HMS; (b) W-HMS, Si/W = 30; (c) W-HMS, Si/W = 30 after 10 reaction cycles; and (d) W-HMS, Si/W = 30 calcined at 873 K after 10 reaction cycles.

in the silica framework as the stretching Si–O vibration mode perturbed by the neighboring metal ions [28,29]. The presence of an infrared band at around 960 cm^{-1} is a piece of direct evidence for the isomorphous substitution of Si by W ions in W-HMS. This result suggests that tungsten species are actually imbedded into the lattice of HMS.

3.2. Catalytic performance of different catalysts

The results of the selective oxidation of CPE to GA over several W-containing catalysts are listed in Table 2. It is found that the GA yield is strongly dependent on the content of the tungsten in the W-containing HMS samples; such a result reveals that the optimum catalyst in the present reaction is that with a Si/W molar ratio at 30. The yield of GA reaches 76%, much higher than that reported previously in this reaction system by using WO_3/SiO_2 or WO_3/TiO_2-SiO_2 as catalysts [8,9]. Moreover, this value is still 5% higher than that reported by using W-MCM-41 as catalyst [10,11]. As we know, this is a big improvement considering the complexity of the reaction system. The result shows much potential for the industrial application of the novel W-HMS catalyst thanks to its huge economic benefits. When the Si/W ratio is higher than 30, a much lower yield of GA is obtained. On the other hand, if the Si/W ratio is as low as 20, inevitable agglomeration of WO_3 and the partial collapse of the mesoporous structure of the W-HMS all lead not only to the lower CPE conversion but also to lower GA yield. A

Table 2
Catalytic performance in the selective oxidation of CPE over various samples[a]

Si/W (mol/mol)	H_2O_2 conversion (%)	CPE conversion (%)	GA yield (%)	Selectivity (%)			
				GA	CPDL	CPLE	Others[b]
∞	0	0	0	0	0	0	0
50	87.6	83.4	55.9	67.0	19.9	10.1	3.0
40	94.0	93.2	66.0	70.8	15.9	8.9	4.4
30	100	100	76.3	76.3	14.6	7.8	1.3
20	85.6	85.9	55.8	65.0	18.3	12.1	4.6

[a] Reaction conditions: 5 mL cyclopentene; 7 mL 50% H_2O_2; 50 mL *t*-BuOH; *T*, 308 K; reaction time 24 h; the reactions were carried out over the catalysts containing the same amounts of W; CPDL, cyclopentan-1,2-diol; CPLE, 2-*t*-butyloxy-1-cyclopentanol.
[b] Others, including cyclopentene oxide, cyclopentenone and cyclopentanone.

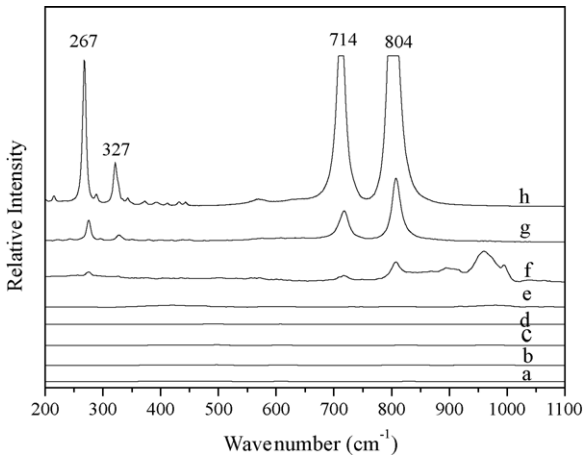

Fig. 5. Raman spectra of bulk WO_3, HMS and W-HMS. (a) pure HMS; (b) W-HMS, Si/W = 50; (c) W-HMS, Si/W = 40; (d) W-HMS, Si/W = 30; (e) W-HMS, Si/W = 30 calcined at 873 K after 10 reaction cycles; (f) W-HMS, Si/W = 30 after 10 reaction cycles; (g) W-HMS, Si/W = 20; and (h) bulk WO_3.

blank experiment with pure silica HMS as catalyst shows that no transformation of CPE to GA could be observed. Furthermore, unsupported pure crystalline WO_3 is also used as catalyst and shows almost no catalytic activity toward the reaction (not shown in the table). The great differences of the catalytic performance among those W-HMS catalysts with different Si/W molar ratios suggest that the presence of the highly dispersed tungsten species in the silica matrix is necessary for the title reaction.

The molar ratio of H_2O_2 to CPE has a substantial effect on the oxidative reaction results. Low GA yield would inevitably result from the incomplete conversion of CPE when the ratio of H_2O_2 to CPE is less than 2:1. If the ratio is higher than 2:1, a co-product, glutaric acid would be produced due to the over oxidation of CPE, which also lead to the low GA yield. As a result, the optimal molar ratio of H_2O_2 to CPE is fixed at 2:1. This value is the same as the theoretically stoichiometric one for the oxidative cleavage of

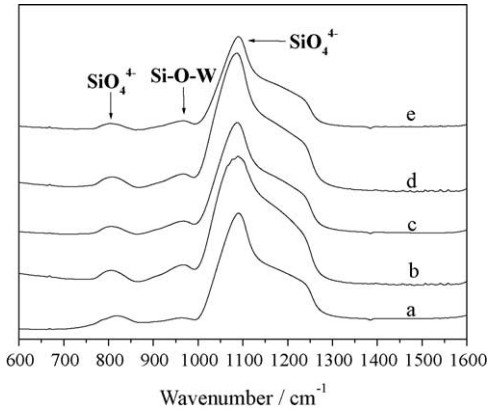

Fig. 6. FT-IR spectra of HMS with the structural Si/W molar ratio as: (a) ∞; (b) 50; (c) 40; (d) 30; and (e) 20.

CPE to GA. The weight content of H_2O_2 in its aqueous solution also has an important effect on the oxidative cleavage of CPE. High H_2O_2 concentration cannot only accelerate the oxidative rate and shorten the reaction time, but also increase the GA yield, which can be ascribed to the decrease yield of the less valuable by-product, cyclopentan-1,2-diol. The complete conversion time for CPE and yield of GA for the 50 wt.% aqueous H_2O_2 are 24 h and 76.3%, while those for the 30 wt.% one are 33 h and 68.2%, respectively. Moreover, almost no decomposition of H_2O_2 to O_2 and H_2O occurred in the above reaction process, after determined by volumetric measurement although no free H_2O_2 could be detected after the reaction. The active oxygen balance in H_2O_2 is established by considering the amount of oxygen converted to the products and the amount of oxygen decomposed to O_2 during the reaction. It is found that there was only 0.6% H_2O_2 decomposed into O_2 and H_2O considering that 10% H_2O_2 was converted to *t*-butylhydroperoxide.

In order to investigate the stability and duration of active W-species in the W-HMS (30) catalyst, the leaching of W-species into the product mixture and the tungsten remaining in the catalyst are also determined after 10 reaction cycles. No detectable leaching of W-species or obvious loss of tungsten in the W-HMS samples could be found, suggesting the presence of strong interactions between tungsten species and the silica-based matrix with HMS structure. The results of the selective oxidation of CPE to GA over W-HMS (Si/W = 30) catalyst with different reaction cycles and the post-regeneration material are listed in Table 3. The GA yield decreases slowly and still stays near 60% after the ninth cycle. After 10 reaction cycles, the used W-HMS (Si/W = 30) catalyst is characterized by WAXS, TEM and laser Raman, as discussed above in Figs. 2, 4 and 5. The results showed that crystalline WO_3 appeared, which might lead to the decrease of the activity. However, the high dispersion of WO_3 and the outstanding catalytic activity could be recovered after calcination at 873 K in air for 2 h, since all the crystalline WO_3 peaks disappeared again, as shown in Figs. 2(d), 4(d) and 5(e) and Table 3, respectively. It is also very interesting that the selectivity toward GA does not decrease obviously along with the repetitions of reaction cycles, suggesting that the decrease of the GA yield should mainly be ascribed to the decrease of the activity. Therefore, the appearance of crystalline WO_3 and the surface contaminant, which must result in the decrease of the active centers, are the main reasons for the decrease of the GA yield. In conclusion, the W-HMS (Si/W = 30) catalyst showed high stability and high activity for the selective oxidation of CPE to GA and could be regenerated by simple calcinations.

In addition, another experiment has been carried out to test whether this novel W-HMS catalyst is actually a heterogeneous one. When the reaction over W-HMS catalyst has been carried out for 10 h, the catalyst is removed through simple filtration and the reaction solution is stirred for

Table 3
Reusability and regeneration of W-HMS (Si/W = 30)[a]

Entry	H_2O_2 conversion (%)	CPE conversion (%)	GA yield (%)	GA selectivity (%)
1	100	100.0	76.2	76.2
2	100	99.0	73.9	74.6
3	100	98.5	72.4	73.5
4	100	96.6	68.9	71.3
5	100	96.0	67.6	70.4
6	100	94.0	68.2	72.6
7	96.0	91.2	64.2	70.4
8	95.6	88.7	63.4	71.5
9	82.8	86.0	59.8	69.5
10	84.6	83.7	57.9	69.2
11[b]	100	98.6	76.1	77.2

[a] Reaction conditions: 5 mL cyclopentene; 7 mL 50% H_2O_2; 50 mL *t*-BuOH; 0.9 g catalyst; T, 308 K; reaction time 24 h.
[b] After regeneration.

another 14 h. No detectable increase of GA yield and CPE conversion in the 14 h of reaction are observed, indicating that the trace amount of leached W species has almost no detectable catalytic effect on the reaction since the leaching of tungsten species from W-HMS (30) is 0.8 ppm in one reaction cycle, as determined by ICP.

4. Discussion

The W-HMS catalyst can be synthesized by using dodecylamine as surfactant molecule at room temperature (~298 K). FT-IR spectra and TEM photos all prove that W has been incorporated into the HMS framework uniformly. The color of W-HMS (Si/W > 30) catalyst is white, indicating that tungsten species is highly imbedded into the matrix of SiO_2. When the Si/W molar ratio is increased to 20, the color of the sample is slightly yellow, suggesting that part of WO_3 is agglomerated on its surface, as confirmed in Figs. 2(f) and 5(g), respectively. The high dispersion of tungsten species in the framework of HMS may contribute to the good performance of W-HMS material for the selective oxidation of CPE to GA by using aqueous H_2O_2 as the oxygen donor. As to the improvement of the GA yield when compared with that of W-MCM-41, the BET surface area of W-HMS is much lower than the area of its counterpart (700 $m^2\ g^{-1}$ versus 1100 $m^2\ g^{-1}$), and the tungsten content is similar (Si/W: 33.6 versus Si/W: 32). The pore size of W-HMS is larger than that of W-MCM-41 (3.1 nm versus 2.6 nm), and the channel length of W-HMS is much shorter than that of the other. In addition, the uniformity of the mesopores of W-HMS is much worse than that of W-MCM-41. It is well known that the diffusion and the mass transfer from the solution to the active centers are very important in a catalytic process. Hence, short channels, unordered mesopores and the large pore size all contribute to the improvement of the catalytic performance.

The W-HMS catalyst exhibits high activity and selectivity in the selective oxidation of CPE to GA. The convenient preparation method and the complete CPE conversion (100%) as well as the high GA yield (76.3%) all make it a promising candidate for its further application in industry. On the other hand, the convenient separation of the W-HMS catalyst from the reaction products mixture, its longer lifetime and simple regeneration method all make it more feasible than the corresponding homogeneous catalysts when applied for industrial use. Moreover, the cheap and plentiful raw materials used in this novel process (one is cyclopentene, originating from a petrochemical by-product, and the other is an environmentally benign aqueous H_2O_2 oxidant) make this process more competitive than the traditional one. Detailed studies on the oxidation mechanism over this novel catalytic material are under way.

5. Conclusions

In this work, a novel W-containing HMS material was synthesized by means of a simple method using TEOS as the source of Si, Na_2WO_4 as W source and dodecylamine as the surfactant; the product showed typical structure of HMS. WO_3 species were highly dispersed into the lattice of the bulk and might be imbedded separately, which could serve as the active centers for the selective oxidation of CPE to GA. The optimal tungsten content was 12.8 wt.% (Si/W = 30) and the GA yield over this catalyst exceeded 76%, much higher values than those reported previously, suggesting its promising potential use in industry.

Acknowledgments

This work was financially supported by the Major State Basic Resource Development Program (Grant no. 2003CB615807), NSFC (Project 20407006), the Natural Science Foundation of Shanghai Science & Technology Committee (02DJ14021), and the Committee of the Shanghai Education (02SG04).

References

[1] S.P. Gorman, E.M. Scott, A.D. Russell, J. Appl. Bacteriol. 48 (1980) 161.
[2] F.M. Collins, J. Appl. Bacteriol. 61 (3) (1986) 247.
[3] H. Furukawa, F. Nishikawa, T. Koyama, Japanese Patent 6,219,548 (1987).
[4] J.F. Deng, X.H. Xu, H.Y. Chen, A.R. Jiang, Tetrahedron 48 (1992) 3503.
[5] X.H. Xu, H.Y. Chen, J.F. Deng, A.R. Jiang, Acta Chim. Sinica 51 (1993) 399.
[6] W.L. Dai, H.K. Yu, A.R. Jiang, J.F. Deng, Acta Chim. Sinica 53 (1995) 188.
[7] W.L. Dai, X.J. Huang, H.Y. Chen, J.F. Deng, Indian J. Chem. 36B (1997) 583.

[8] R.H. Jin, X. Xin, W.L. Dai, J.F. Deng, H.X. Li, Catal. Lett. 62 (1999) 201.
[9] R.H. Jin, H.X. Li, J.F. Deng, J. Catal. 203 (2001) 75.
[10] H. Chen, W.L. Dai, J.F. Deng, K.N. Fan, Catal. Lett. 81 (2002) 131.
[11] W.L. Dai, H. Chen, Y. Cao, H.X. Li, S.H. Xie, K.N. Fan, Chem. Commun. 7 (2003) 892.
[12] C.W. Guo, W.L. Dai, Y. Cao, S.H. Xie, K.N. Fan, Acta Chim. Sinica 61 (2003) 1496.
[13] P.T. Tanev, M. Chibwe, T.J. Pinnavaia, Nature 368 (1994) 321.
[14] R.T. Yang, T.J. Pinnavaia, W. Li, W. Zhang, J. Catal. 172 (1997) 488.
[15] T.R. Pauly, Y. Liu, T.J. Pinnavaia, S.J.L. Billinge, T.P. Rieker, J. Am. Chem. Soc. 121 (1999) 8835.
[16] A. Tuel, Microporous Mesoporous Mater. 27 (1999) 151.
[17] R. Mokaya, W. Jones, Chem. Commun. (1996) 981.
[18] A. Tuel, S. Gontier, R. Teissier, Chem. Commun. (1996) 651.
[19] S. Gontier, A. Tuel, Microprous Mater. 5 (1995) 161.
[20] Z. Fu, J. Chen, D. Yin, L. Zhang, Y. Zhang, Catal. Lett. 66 (2000) 105.
[21] H. Yamashita, K. Yoshizawa, M. Ariyuki, S. Higashimoto, M. Che, M. Anpo, Chem. Commun. (2001) 435.
[22] Y. Liu, K. Murata, M. Inaba, Chem. Lett. 32 (2003) 992.
[23] Y. Liu, K. Suzuki, S. Hamakawa, T. Haykawa, K. Murata, T. Ishii, M. Kumagai, Catal. Lett. 66 (2000) 205.
[24] Y. Liu, K. Murata, M. Inaba, N. Mimura, Catal. Lett. 89 (2003) 49.
[25] Y.C. Xie, Y.Q. Tang, Adv. Catal. 37 (1990) 1.
[26] J.G. Graselli, B.J. Bullkin, Analytical Raman Spectroscopy, Wiley, New York, 1991, p. 352.
[27] Z.R. Zhang, J.S. Suo, X.M. Zhang, S.B. Li, Appl. Catal. A: Gen. 179 (1999) 11.
[28] V. Parvulescu, C. Snastasescu, C. Constantin, B.L. Su, Catal. Today 78 (2003) 477.
[29] P. Wu, T. Tatsumi, T. Komatsu, T. Yashima, J. Catal. 202 (2001) 245.